11 R.5 RADAR VELOCITY VARIANCE AND HYDROMETEOR CLASSIFICATION

Raquel Evaristo*, Georges Scialom and Yvon Lemaître

CETP/IPSL-CNRS-UVSQ, Vélizy, France.

1. INTRODUCTION

[1]

The present paper deals with the variance obtained as the third moment of the spectrum calculated by FFT in the radar Ronsard (Nutten et al, 1979), and more specifically aims at giving an interpretation of the variance in the particular case of vertical scanning (i.e the "vertical" contribution). Indeed, if accurately calculated, the variance σ_D^2 of the observed velocity (i.e. the velocity along the radar beam) could be of great scientific interest as shown later.

The various contributions to the variance ("horizontal" and "vertical") depend in particular of the angle of elevation of the radar beam with respect to the horizontal and are recalled in section 2, along with the method of analysis of the variance data. Results on a case study of stratiform precipitation observed during the MAP experiment (Bougeault et al, 1000), are presented in section 3. Section 4 relates to two other case studies of MAP and in particular to a convective event. Finally, the conclusion also contains some ideas of future experiments and/or algorithms to validate and extend these first results.

2. MEASURED VARIANCE ANALYSIS

The variance σ_D^2 of the observed velocity (i.e. the velocity along the radar beam hereafter called the "variance") contains several contributions, namely (see Doviak et Zrnic, 1984 ; Chapman et Browning, 2002):

$\sigma_D^2 = \sigma_s^2 + \sigma_r^2 + \sigma_f^2 + \sigma_t^2$ where :

σ_f^2 is the contribution due to the terminal fall velocity of hydrometeors;

σ_s^2 is the contribution due to the wind shear (and /or to the effect of large energy eddies) (Atlas et al, 1969) ;

σ_r^2 is the contribution due to antenna rotation ;

σ_t^2 is the contribution due to the turbulence within the sampling volume.

The present study focuses on σ_f^2 whose contribution is maximum at the vertical and we show further that other contributions, rather "horizontal" in essence can be independently estimated or neglected for the chosen experimental cases.

The data set used here to perform tests on the variance is extracted from data obtained during the MAP experiment. Recall this international experiment aimed at scrutinizing the role of the Alps in triggering and organizing precipitation in the Po Plain (Northern Italy) gathered a great number of instruments and involved simultaneous processing of several numerical models. Concerning the instruments, particular importance was given to three Doppler radars, namely the Swiss Meteorology operational radar of Monte-Lema, the French C-band Doppler Ronsard, and the US S-band Dual Polarization Doppler radar. During the whole field phase (autumn 1999), all radars worked properly and allowed many precipitation events to be observed, among which several were stratiform. All data analysed in the present paper come from the Ronsard data bank. In this radar, FFT are performed for 512 gates 200 m spaced apart, and the first three moments (reflectivity, wind velocity and variance) of the spectrum are recorded. Many volumetric conical sequences performed within stratiform precipitation were recorded. These sequences (always of the same type in the present paper) consisted of 20 consecutive cones at increasing elevations from 0.1 up to 69.4 degrees. These elevations were chosen in order to best fulfil the space. Although measurements at the radar vertical (elevation = 90 degrees) would have been ideal for the purposes of the present paper, we used data

* *Corresponding author address* : Raquel Evaristo, CETP-CNRS-UVSQ, 10-12 Avenue de l'Europe, 78140 Vélizy, France;
e-mail: evaristo@cetp.ipsl.fr

obtained at elevation 69.4 degrees (the maximal elevation available in the sequences programmed during the MAP experiment). This of course induces an additional error due to the residual contribution of the horizontal wind, as further discussed in the present section.

The choice of stratiform precipitation in the whole data set for testing the method had several advantages in terms of simplicity for data interpretation. First, conditions are changing slowly, so that measurements from one sequence to the next one also changes slowly, leading to looking at many successive sequences with smoothed variations of the mean reflectivity and the mean velocity fields (the latter can be considered as linear). Second, the frequent presence of a bright band allows clear distinction of the phase (solid or liquid) of the hydrometeors responsible for radar backscattering (the radar signal). In these conditions, one can expect easier interpretation for the variance of the velocity (the third moment).

The method used for data analysis is the following:

First, a day is selected during which radar data from stratiform precipitation have been recorded for a long time period. Thus, several successive volumetric conical sequences are selected.

For each sequence, a VAD processing of the whole scanned volume allows obtaining the vertical profile of the three wind components, and of the terminal fall velocity of the HM (Testud et al, 1980). In this case, data from all elevations are processed. Averaging reflectivity within each horizontal plan provides the vertical profile of the mean reflectivity.

As for the variance, its mean vertical profile is also obtained by averaging data within each horizontal plane, but, since no scan was done at elevation 90 degrees (the radar vertical), only data at elevation 69.4 degrees (the highest available) are retained to strongly reduce the contamination by other variance contributions, as seen now: Fall velocity contribution to variance σ_f^2 is modulated by $\sin^2$[elevation (in degrees)] = $\sin^2 69.4$, = 0.875, while "horizontal" contributions are modulated by $\cos^2(69.4) = 0.124$.

The contribution due to antenna rotation σ_r^2 is at worst only 0,01 $m^2 s^{-2}$, i.e. $\sigma_r \sim$ 0,1 $m s^{-1}$ at elevation 69.4 degrees.

The contribution due to the turbulence within the sampling volume σ_t^2 can be estimated from the variance measured at low elevation (less than 10 degrees). We find a value about 0,6-0,9 $m^2 s^{-2}$ at low altitude (within rain). Within ice, it should be even smaller. When this turbulence is "projected" at high elevation, the corresponding variance contribution is [0.6-0.9] x $\cos^2$ (69.4)/$\cos^2$ (10) = 0.124/0.970 ~ 0.08-0.12 $m^2 s^{-2}$. If the turbulence was of equal importance horizontally and vertically, the corresponding contribution would be stronger [0.6-0.9] $m^2 s^{-2}$.

The contribution σ_s^2 due to the wind shear (effect of large energy eddies) is probably negligible outside frontal surfaces: a shear 2 m/s on the horizontal wind due to the arrival of cold front, would result in 2 m/s standard deviation of the wind which, projected onto the vertical , yields 0.7 $m s^{-1}$, that is $\sigma_s^2 \sim 0.5\ m^2 s^{-2}$. In case of no wind shear, $\sigma_s^2 \sim 0.1\ m^2 s^{-2}$ (limit due to measurement error).

The total contribution to the "horizontal" variance (without that of V_f) may be estimated as 0.2-0.3 $m^2 s^{-2}$.

Note that averaging velocity or reflectivity data provides mean values which represent the first order solution of the corresponding quantities. Similarly, averaging variances within a horizontal plane provides the mean spectral width of the Doppler spectrum since the variance of mean value of a parameter is the mean of the individual variances of this parameter (see Appendix).

Still, the variance can be highly variable, due to the heterogeneousness and to the variability of the population of HM. This the reason why after considering the mean variance in subsection 3a, a more detailed (second order) analysis of the results, based upon the histogram of the variance is given in subsection 3b.

3. APPLICATION TO MAP IOP 10 (24 OCTOBER 1999)

The Intensive Observation Period (IOP) 10 was studied from 0615 to 1630 (all times UTC). There is no precipitation at 0615, then appears a layer with precipitation between 0630 and 0700, but only above 3000 m (in solid phase). The period 0715-1145 is characterized by stratiform precipitation up to 6-8 km height, then appears a precipitation–free layer at 3-4 km, approximately, from 1200 to 1315, then from 1330 until 1630, precipitation is progressively confined to the lower two kilometres. The whole studied period totalizes 41 sequences (since the Ronsard radar

scanned a volumetric sequence each 15 minutes), so that for these sequences, vertical profiles of terminal fall velocity V_f of HM, mean reflectivity REF and mean variance VAR are available. We select here the time period during which stratiform precipitation is continuous (0715-1145).

3.1 Mean variance

Figs. 1a-f show vertical profiles of terminal fall velocity, mean variance and mean reflectivity at six consecutive times. The sequences shown in Fig. 1 refer to the period 1045-1200.

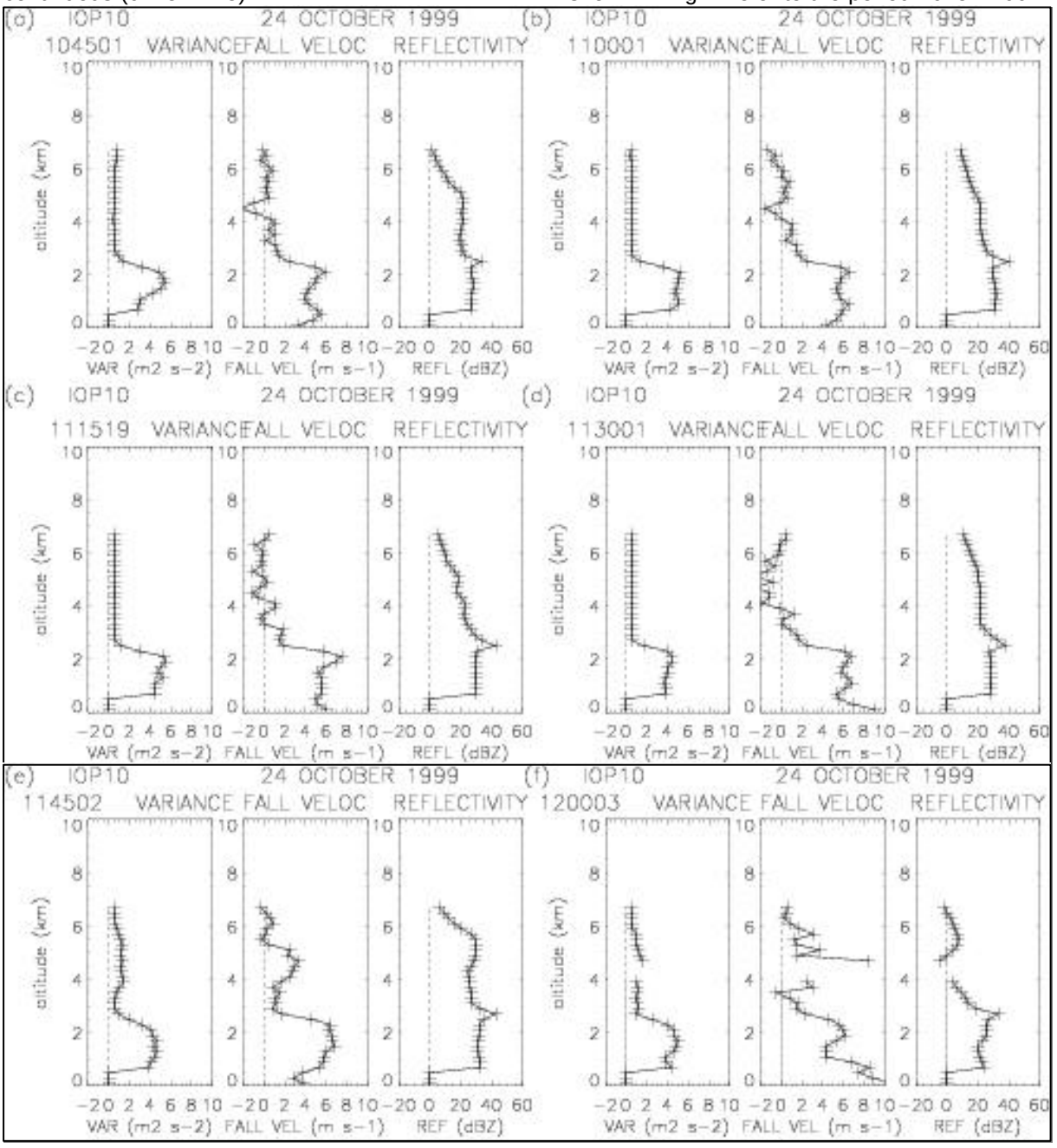

Fig. 1 Vertical profiles of variance, fall velocity and reflectivity on 24 October 1999 (IOP10)

On **Fig. 1** the V_f profiles exhibit the classical distinction between rain (liquid phase), below the 0°C isotherm, and the ice phase, above. The REF profile clearly shows a bright band feature (reflectivity maximum just below the 0° isotherm).

Within the ice phase, one can see at 1145 and 1200 UTC (Figs. 1ef) about 5000 m altitude, a

local increase of the fall velocity, about 3 m s-1 instead of 0.5-1 ms-1. **Fig.1** also shows VAR profiles, which has different characteristics above and below the 0°C isotherm: above the 0°C isotherm, the variance in ice phase is low, generally 0.5 m^2 s^{-2}, which is expected since, on the one hand, ice particles fall with velocity 0-2 m s^{-1}, on the other hand the maximum variance of the various ice particles fall velocities is about 1 m^2 s^{-2}. Thus within the ice phase, these small variations of the variance are generally very small and not easily detected, while the corresponding V_f variations are. However, the 1145 profiles (Fig.1e) for which V_f reaches 3 m s^{-1} induces a variance increase up to 1 m^2 s^{-2} which is visible on the variance profile, but this case, which could correspond to the existence of a graupel layer, is a favourable one. This interpretation is completed further in the next subsection.

Below the 0°C isotherm, the fall velocity is about 6 ± 2 ms-1, typical of raindrops, while the variance increases significantly (compared to the ice area), with values such as 3.5-5 m^2 s^{-2} (for example at sequences between 0845 and 1015). This means that the standard deviation (s. d.) of the wind is 2 ± 0.2 m s^{-1}.

This is consistent with the presence of raindrops with diameters in the range 1-1.8 mm (Mason, 1971).

3.2 Variance histogram

A second order analysis of the parameter "variance" relying upon the histogram of the variance is then performed at each altitude (in fact at each altitude slice 200 m width). This histogram is built in the following way: 10 classes of variance are represented namely, 0-0.25, 0.25-1, 1-2, 2-3, 3-4, 4-5, 5-6, 6-7, 7-8, 8-9 (in m^2 s^{-2}). These classes are first calculated in numbers (number of points of the given class in a given horizontal plane) then converted in percentages of the same points under the same conditions and plotted in isolines. The examples displayed **Figs. 2af** correspond to the cases displayed on **Figs 1af**, and clearly exhibits three regions (rain, mixed phase and snow).

The snow region above the 0°C isotherm (at 2.7 km) is characterized by an unimodal spectrum in 50-60 % of the cases (variance = 0.25 m^2 s^{-2} in most of them), but a significant percentage 40-50 % concerns class 2 (0.25-1 m^2 s^{-2}) and sometimes class 3 (1-2 m^2 s^{-2}). Between 1130 and 1145 UTC, the variance histogram jumps from 2 to 3 m^2 s^{-2}, which could mean that one (or several) more HM with higher terminal fall velocities are significantly present (Figs 2de). This could be the signature of the presence of graupels in the considered layer as suspected in the previous paragraph.

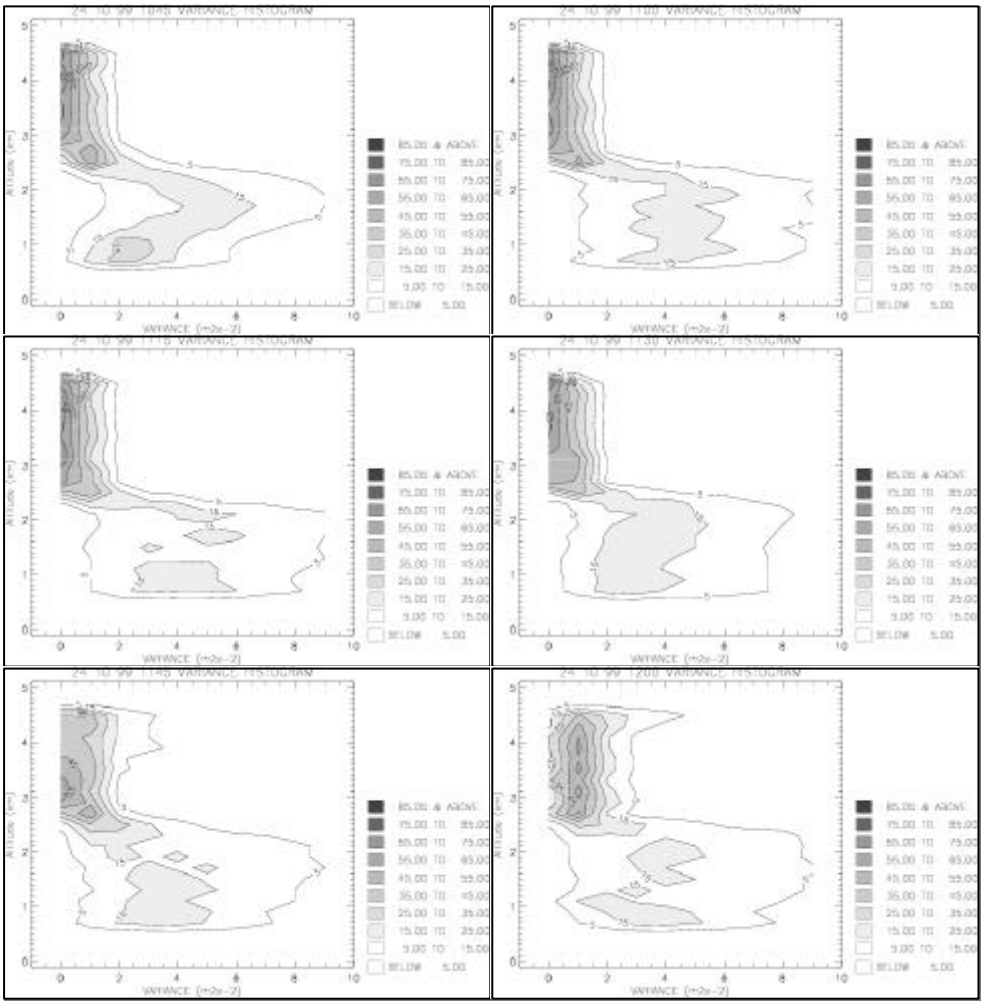

Fig. 2 Variance histogram for 24 October 1999 for the same times as Fig. 1

The mixed phase region is apparent below 2.5 km with a mean variance 0.6 m^2 s^{-2}. At 2.1 km and 1.9 km, the variance increases (0.7 and 2.3 m^2 s^{-2}, respectively), and its histogram widens. In the present case, these two altitudes sign the transition due to the melting layer

The rain region is characterized by a considerable enhancement of the variance and of the classes of variance which define the variance histogram. All classes are concerned and the most populated class varies with altitude: at 1 km, 15-25% of the points have variance 2-4 m^2 s^{-2} .

4. OTHER CASES

Other IOPs characterized by stratiform precipitation, namely IOP 6 (13 October 1999), IOP 8 (20 10 1999), IOP 14 (4 November 1999) were studied in the same way as IOP 10, and exhibit similar profiles for V_f and the velocity variance. In those cases too, the variance varies dramatically from the rain region 4-6 $m^2 s^{-2}$, to the snow region 0-1 $m^2 s^{-2}$, also in good correlation with the changes in the terminal fall velocity (4-10 m s^{-1} below, 0-2 m s^{-1} above the 0°C isotherm, respectively). See Fig. 3 **(**13 October 1999/IOP 6) profiles.

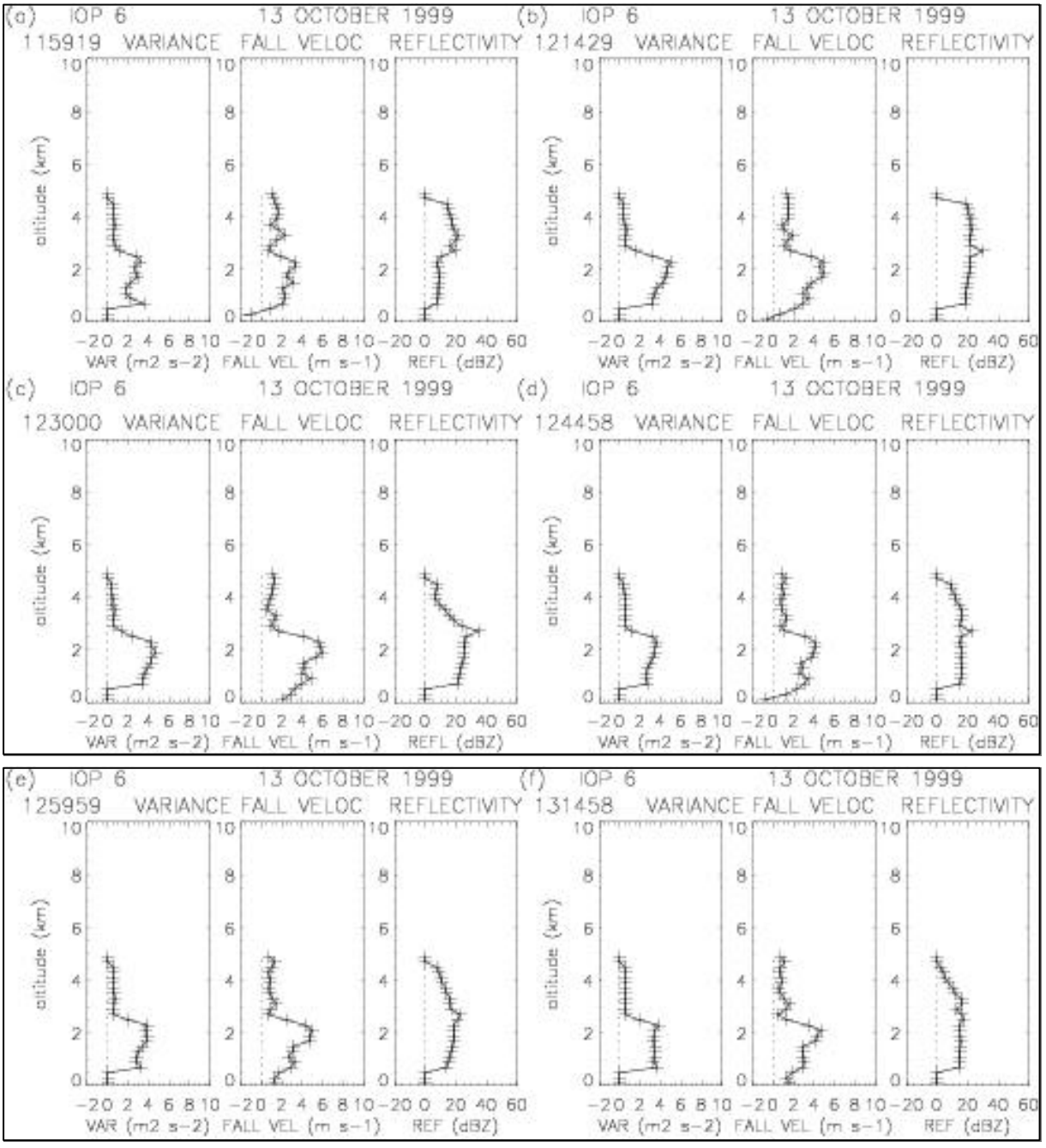

Fig. 3 Vertical profiles of variance, fall velocity and reflectivity on 13 October 1999 (IOP6)

The presence of graupels is suggested by an enhancement of the terminal fall velocity (from 1 m s^{-1} in snow to 2 m s^{-1} in graupels) but its signature on the mean variance is very tiny and not really visible on the profiles. It is however visible on the histogram of the variance, which shows a tendency to spread out toward higher values, which may be interpreted as the presence of hydrometeors with higher fall velocities mixed with classical snowflakes with slower fall velocities. This is visible in the case of IOP 6 at 1214 and 1245 (Fig. 4ab): there is a light enhancement of the variance width on the variance histogram at 1215 at 3500m altitude, which is not present at 1245. IOP 8 (20 October 1999) at 0600-0715, and of IOP 14 (4 November 1999) at 1115-1300 show similar layers with enhanced V_f and velocity variance (variance histograms not shown for these cases). The variance is also a good tracer of the passage rain-snow even in the case of very light precipitation as seen on the example of IOP 16 (11 November 1999, not shown).

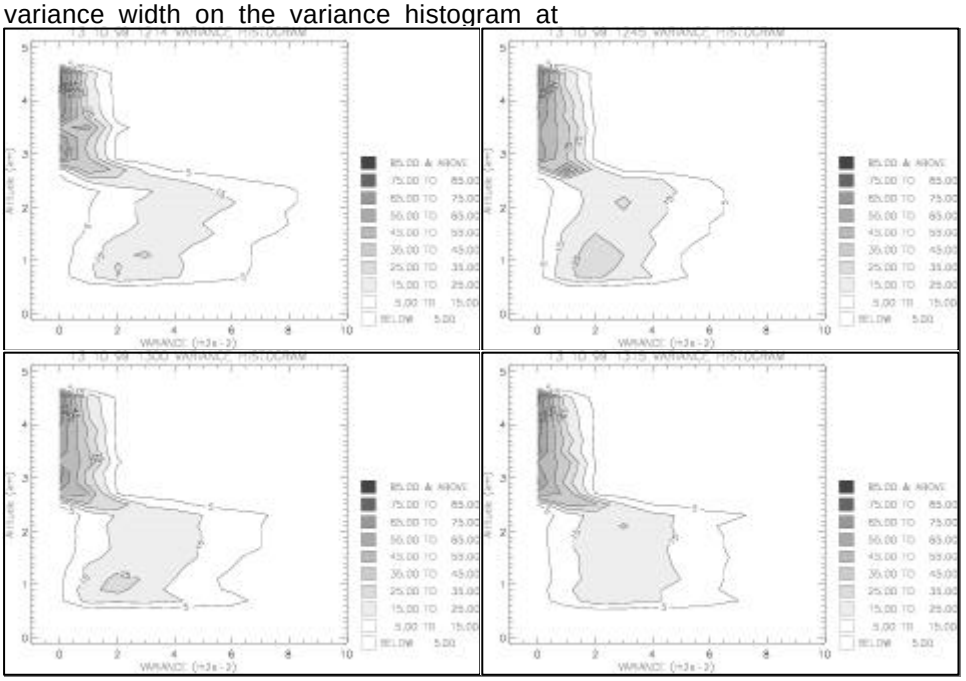

Fig. 4 Variance histogram for 13 October 1999 (corresponds to Fig. 3)

A particular point must be made on IOP2A (17-18 October 1999), characterized by observed convective rain and hail. In that case, a frontal rain band initialised and organized at the mesoscale as a SW-NE squall line crossing the Alps toward the Southeast, and another band triggered by the local orography along the same direction merged together when they came close to each other. Hail appeared during this phase of merging, and the resulting band, initially bi-dimensional as long as it was over the Alps turned to a three dimensional structure when reaching the Pô plain. Hail was identified from 1930 to 2030 by applying the algorithm for hydrometeor identification of Zrnic et al (2001) to data of the US S-POL polarimetric radar which was working in coordination with the RONSARD and Monte Lema radars. Figs. 5a-d show fall velocity and variance profiles between 2045 and 2200. Evolution from stratiform (at 2045 UTC) to convective (from 2145 UTC) precipitation is apparent. Mean reflectivity increases from 20 to 40 dbZ. The variance profile which is still "stratiform" at 2045, with 2 regions with strong variance below the 0°C isotherm and weaker variance above, becomes progressively homogeneous with altitude, with very strong values probably indicative of the presence of hail. Battan and Theiss (1972) who observed particles with a vertically-pointing X-band radar, report velocity spectra of hail are characterized by variances ranging from 3 to 12 $m^2 s^{-2}$. The profiles of variance histograms also show such a tendency during the same period (Fig. 6).

The variance profile with altitude seems to be a good indicator for separating convective from stratiform areas.

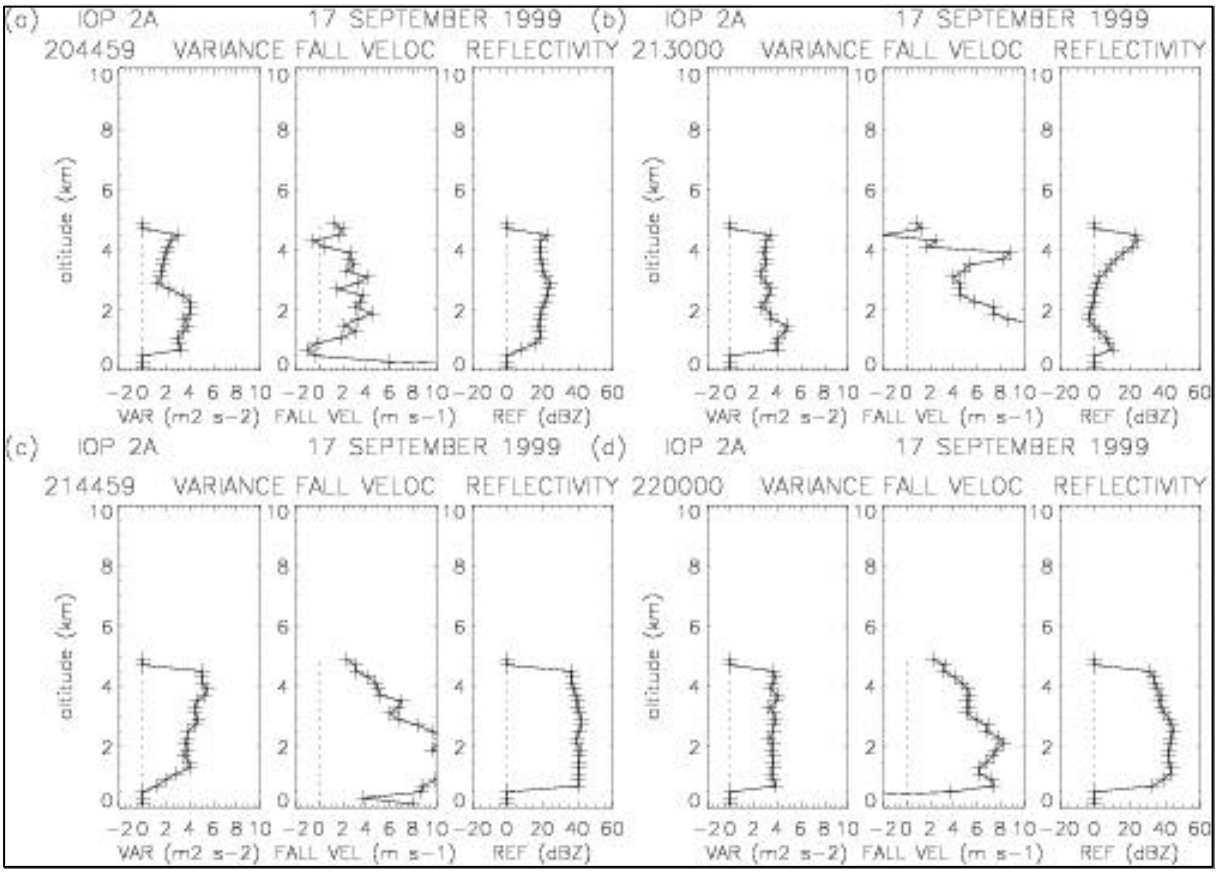

Fig. 5 Vertical profiles of variance, fall velocity and reflectivity on 17 September 1999 (IOP2A)

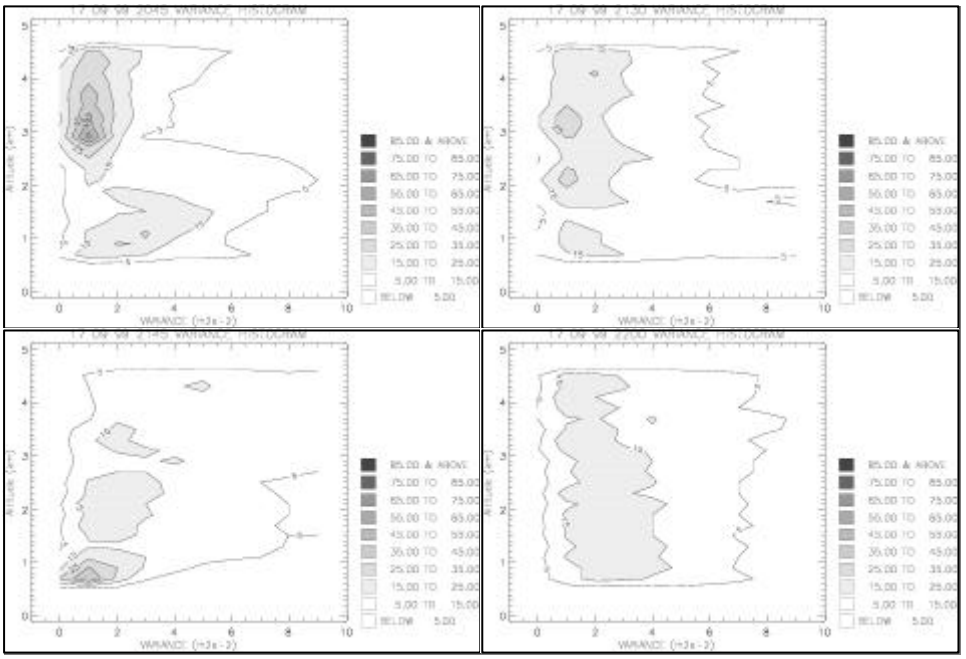

Fig. 6 Variance histogram for 17 September 1999 (corresponds to Fig. 8)

5. CONCLUSION AND PERSPECTIVES

The present study has illustrated the usefulness of the parameter "velocity variance", at least in stratiform precipitation. It has first shown that in such situations, the variance could be used in order to discriminate the liquid precipitation region from the solid precipitation region, by simple inspection of the mean profile of variance as a function of altitude at high elevation (preferably at vertical incidence). The obtained profiles agree fairly well with the terminal velocity profiles which need that a complete volumetric sequence be processed. Second, the analysis of the variance histogram has shown that in the liquid region, the variance could help providing the raindrop size distribution by simple examination of the mean terminal fall velocity and of the standard deviation of the various classes of velocities about this velocity. In the solid phase region, the histogram (with generally fewer classes with smaller variances) could help identifying HM with greater V_f such as graupels. The particular case of hail rather concerns convective precipitation areas, but it was also shown in this paper that the variance had a clear signature as shown by Battan and Theiss (1972).

HM classification by radar uses the polarimetric observables obtained by means of dual polarization radars. Such is the case for the classification proposed by Zrnic et al (2001) in which a fuzzy logic algorithm provides for each measurement, which HM (out of a list of 11) is the most likely to be present. Since these algorithms are improved by the knowledge of a temperature profile (not always available), they should be also improved by additional kinematic information such as the terminal fall velocity of HM and/or the variance velocity (measured at the vertical of the radar), and even the variance histogram, at least within stratiform precipitation.

Appendix

Let a parameter $M= (M_1+M_2+ \ldots +M_N)/N$
with $\sigma^2 (M_I) = \text{Constant} = \sigma^2$ $(I = 1, 2, \ldots, N)$

Then: $\sigma^2 (M) = N \sigma^2 (M_I) /N^2 = \sigma^2 /N$

(A1)

In the general case, M is a weighted mean but Eq.A1 generally remains a good approximation In that case, if again: $\sigma^2 (M_I)$ = constant $=\sigma^2$, then:

$M= (\lambda_1 M_1+\lambda_2 M_2+ \ldots +\lambda_N M_N)/ (\lambda_1+\lambda_2+ \ldots +\lambda_N)$

$\sigma^2 (M) = \Sigma[(\lambda_I^2 \sigma^2 (M_I)] / (\lambda_1+\lambda_2+ \ldots +\lambda_N)^2 = \sigma^2 \Sigma[(\lambda_I^2] / (\lambda_1+\lambda_2+ \ldots +\lambda_N)^2$ (A2)

As an example, if $\lambda_1=1$; $\lambda_2 =2$; … $\lambda_N =N$, then

$\sigma^2 (M) = \sigma^2 \Sigma[(1^2+2^2+\ldots N^2)] / (1+2+\ldots+N)^2 = (2/3) (2N+1) \sigma^2 / N(N+1)$ (A3)

For great N, $\sigma^2 (M) \tilde{} (4/3) \sigma^2 / N$ of the same order of magnitude as $\sigma^2 (M)$ given by Eq. A1.

If $\sigma^2 (M_I)$ is not constant, one may define a constant $\sigma^2 = \lambda_I^2 \sigma^2(M_I)$ with $0< \lambda_I^2 < 1$

Then $\sigma^2 (M) = \Sigma[(\lambda_I^2 \sigma^2 (M_I)] / (\lambda_1+\lambda_2+ \ldots +\lambda_N)^2 = N \sigma^2 /(\lambda_1+\lambda_2+ \ldots +\lambda_N)^2$ (A4)

If no λ_I are smaller then 0.5, then $\sigma^2 /N < \sigma^2 (M) < 4 \sigma^2 /N$ (A5)

References

Atlas, D. , R. C. Srivastava and P. W. Sloss, 1969: Wind shear and reflectivity gradients effects on Doppler radar spectra.II. *J. Appl. Meteorology*, **8**, 384-388.

Battan, L.J., and Theiss, J. B., 1972: Observed Doppler of spectral hail. *J. Appl. Meteorology*, **12**, 1001-1007.

Bougeault, P., P. Binder, A. Buzzi, R. Dirks, R. Houze, J. Kuettner, R. B. Smith, R. Steinacker, H. Volkert and all the MAP scientists, 2001: The MAP Special Observing Period. *Bull. Amer. Meteor. Soc.*, **82**, 433-462.

Chapman, D., and K.A. Browning, 2001: Measurements of dissipation rate in frontal zones. *Quarterly J. Royal Meteor. Soc*., **127**, 1939-1959.

Doviak , R. J. and D. S. Zrnic, 1984: Doppler radar and weather observations, Academic Press, 458 pp.

Mason, B. J., 1971: *The Physics of clouds.* Clarendon Press, 671 pp.

Nutten, B., P. Amayenc, M. Chong, D. Hauser, F. Roux and J. Testud, 1979: The RONSARD radars: A versatile C-band dual Doppler facility, *IEEE Trans. Geosc. Electron.*, **GE 17**, 281-288.

Sirmans, D, and B. Bumgarner, 1975: Estimation of spectral density mean and variance by covariance argument techniques. *16th Conf. Radar Meteor.* , Houston, TX, Amer. Meteor. Soc., 6-13.

Sloss, P. W., and D. Atlas, 1968: Wind shear and reflectivity gradients effects on Doppler radar spectra. *J. Atmos. Sci*., **25**, 1080-1089.

Testud, J., G. Breger, P. Amayenc, M. Chong, B. Nutten and A. Sauvaget, 1980: A Doppler radar observation of a cold front. Three dimensional air circulation, related precipitation system and associated wave-like motions. *J. Atmos. Sci.*, **37**, 78-98.

Zrnic, D. S., A. Ryzhkov, J. Straka, Y. Liu, and J. Vivekanandan, 2001: Testing a procedure for automatic classification of hydrometeor types. *J. Atmos. Oceanic Technol.,* **18**, 892-913.